XVII[èmes] Journées Nationales Génie Côtier – Génie Civil
Chatou, 2022
DOI:10.5150/jngcgc.2022.009 *© Editions Paralia CFL*
disponible en ligne – http://www.paralia.fr – available online

Seasonal runup variability at a reef-lined beach: field assessments in the Caribbean

Thibault LAIGRE [1,2], Yann BALOUIN [3], Alexandre NICOLAE-LERMA [4], Nico VALENTINI [3], Deborah VILLARROEL-LAMB [2], Manuel MOISAN [1], Ywenn DE LA TORRE [1]

1. BRGM Guadeloupe, Parc d'activités Colin, La Lézarde, 97170 Petit Bourg, Guadeloupe, France.
   t.laigre@brgm.fr
2. University of the West Indies, St Augustine Campus, Trinidad and Tobago.
3. BRGM Occitanie-Université de Montpellier, 1039 Rue de Pinville, 34000 Montpellier, France.
4. BRGM Nouvelle-Aquitaine, Parc technologique Europarc, 24 Av. Léonard de Vinci, 33600 Pessac, France.

Abstract
The proposed article deals with the assessment of coral reef impact on runup-induced coastal flooding over a two years and 10 months period at Anse Maurice, a reef-fringed pocket beach located at Guadeloupe Island, in the Caribbean region. The reef is mainly constituted by complex structures of Acropora Palmata dead colonies. Daily maximum marine inundation was assessed using a fixed video system. Daily Highest Runups (DHR) remains primarily correlated to individual storm event as extreme runups are observed in correlation with storm swells. However, storm runup intensity is highly modulated by the non-astronomic annual periodicity of sea level (24% of the global runup variability) showing minima in Mars and maxima in October. Those variabilities determine the sea surface elevation and thus water depth over the reef. Yet, reef submergence is known to be an important parameter involved in wave transformation over reefs. The later itself is due to sudden bathymetric loss and high bottom roughness typical of reef environments. This leads to different runup response for similar incident wave conditions. For example, most of the winter storm events only induce moderate intensity runup (mainly due to lower water level controlled by the seasonal sea level cycle) while cyclonic events with the same swell intensity generate more extreme runups. This study brings new comprehensive elements on runup behaviour and nearshore processes at different timescales on reef-lined beach.

Keywords: Caribbean, Video monitoring, Coral reefs, Runup, Sea level.

1. Introduction

Small Caribbean Islands are highly vulnerable to coastal flooding with maximum coastal flooding events related to cyclones (RUEDA *et al*., 2017) Extreme sea-levels and direct wave impact are the principal parameters involved in coastal inundation. Short-term mean sea-level variability is related to both predictable parameters (e.g., tidal cycles) and stochastic parameters (e.g., wave and wind setup, storm surge). Sea-level fluctuations on a yearly basis are also well-known and may be the consequence of the association of seasonal variations of atmospheric pressure and winds, steric effect, ocean circulation (TORRES & TSIMPLIS, 2012) and water mass transfer from the continents (ice sheets, glaciers or rivers).

Furthermore, there is strong evidence that healthy coastal ecosystems, and in particular tropical ecosystems, can substantially reduce coastal hazards (e.g. GUANNEL *et al*., 2016). At reef-lined coasts, the attenuation of the impact of coastal hazards depends mainly on coral reef morphology (e.g., slope, width, structural complexity) whose main effect is the dampening incident wave energy and hydrodynamic forcing (e.g., water level). Wave propagation on coral reefs produce a tremendous energy dissipation (HARRIS *et al*., 2018). A meta-analysis conducted by FERRARIO *et al*., 2014 estimated that coral reef assemblages dissipate an average of 97% of incident wave energy at the shoreline, even if their results remained site-specific.

Modelling approaches of runup at reef-lined coast were published recently (PEARSON *et al*., 2017; QUATAERT *et al.,* 2020) and they pointed out the lack of field observations to properly calibrate or validate the models. This study investigates runup field observations obtained by video monitoring at the scale of the year with the objective to identify the key parameters involved in runup processes and their relative contribution.

2. Material and methods

2.1 Study site

Anse Maurice is located in Guadeloupe Island (France) in the Lesser Antilles (figure 1 (a) and (b)). It is a small beach about 200 m long and between 5 and 20 m wide.

The beach is bordered by a fringing reef mainly composed by *Acropora Palmata* dead colonies covered by algae. However, some complex structures of several meters in height are still observed. The boundary between the reef and the lagoon is unclear, as many coral formations are visible near the shoreline level. In the southern part of the site, an eastward channel is identifiable where the coral structures are sparser and deeper (figure 1 (b)).

The Anse-Maurice site is a wave-dominated beach where offshore swells vary greatly with an annual mean of 1.2 m. It is exposed to strong Atlantic swells with most of the storms occurring during the winter season from December to March; these swells mainly comes from the North to East-North-East direction.

The site is also subject to cyclonic events from July to November which can generate the most powerful waves reaching the island. Nevertheless, due to the site exposition, only swells from North to East direction impact it directly. Besides these two highly energetic wave regimes, waves generated by the trade winds affect the region all year round with wave heights ranging from 0.5 to 2 m (REGUERO *et al*., 2013). The flooding risks are primarily associated with the occurrence of tropical cyclones (KRIEN *et al*., 2015; RUEDA *et al*., 2017).

The area shows a semi-diurnal microtidal range, with diurnal and mixed inequality, a mean amplitude of 0.25 m and ranging from 0.1 m during neap tides to 0.7 m during spring tides (SHOM, 2020).

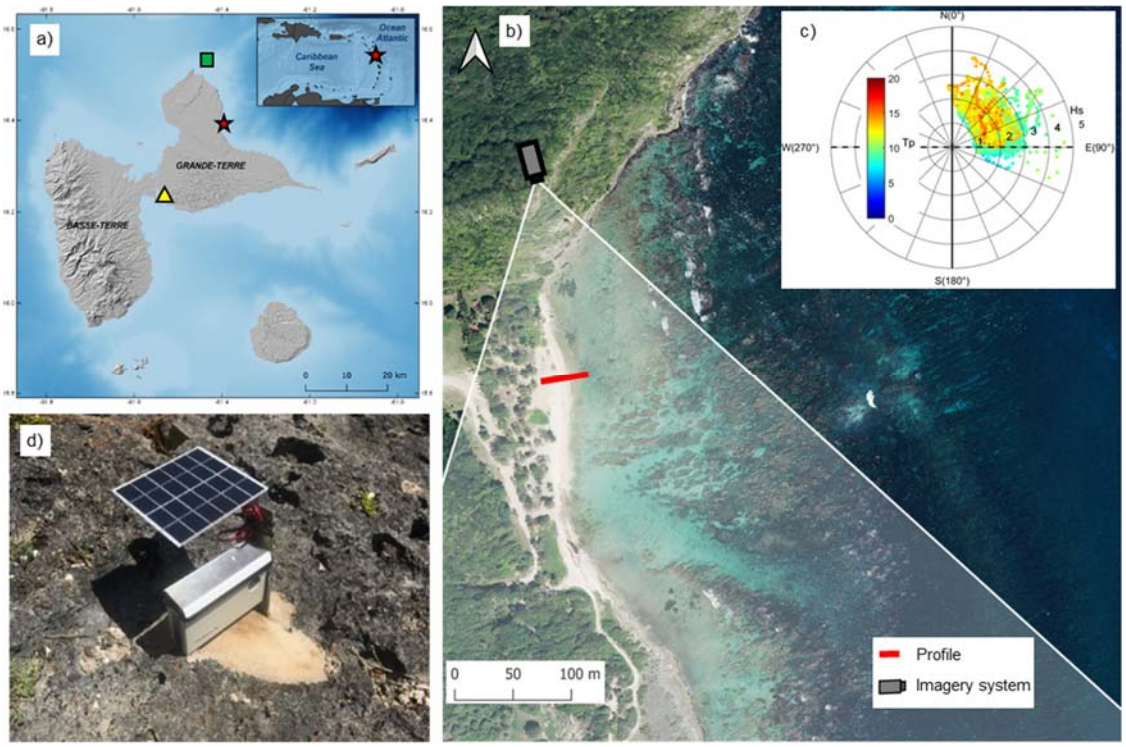

Figure 1. (a) Location of Guadeloupe Island in the Caribbean and Anse-Maurice beach (red star) at the East of the Island. Pointe-à-Pitre tide gauge (yellow triangle). (b) Anse-Maurice beach orthophotography. (c) Wave rose for the period of the study extracted from MARC model. (d) Imagery system installed at Anse-Maurice.

Seasonal sea-level changes are the combined result of atmospheric pressure variations, wind effect and steric expansion. Atmospheric pressure annual variations in the Caribbean are the consequence of Inter Tropical Convergence Zone (ITCZ) displacement. Surface winds are dominated by the Trade winds and steric expansion which is due to temperature, salinity and pressure change of seawater (TORRES & TSIMPLIS, 2012). The wind effect is hard to detect as it is greatly site-specific at the opposite of steric expansion which is generated in large water masses. In Guadeloupe Island in particular,

the barometric effect is not significant (< 0.01m) and most annual sea-level variations are the consequence of steric effects with an amplitude of 0.15 m in Guadeloupe Island, maxima on October and minima in April (TORRES & TSIMPLIS, 2012).

2.2 Field measurements

Video derived coastal state indicators

Video systems are widely used to evaluate coastal evolution and coastal hydrodynamics allowing the quantitative acquisition of optical signatures of shoreline position, nearshore morphologies, wave characteristics, or wave runup (e.g. AARNINKHOF, 2004; HOLMAN & STANLEY, 2007). Recently, low-cost webcams are increasingly used (ANDRIOLO *et al*., 2019; VALENTINI *et al*., 2020) and have proven their ability to acquire reliable data at an affordable price.

In this study, a low-cost Solarcam© camera system was implemented in April 2019 to monitor coastal evolution (figure 1 (b) and (c)). Each system comprises an 8 MP resolution smartphone protected by a waterproof housing, and powered by a solar panel. The whole system is entirely autonomous as it is programmed to record an image every 10 minutes. This low-cost device showed its applicability on several purposes (VALENTINI & BALOUIN, 2020; MOISAN *et al*., 2021).

A dataset of 2.5 years and 10 months has been analyzed in this study. The images from the cameras were calibrated with ground control points using the HOLLAND *et al.* (1997) methodology in order to obtain data in real-world scale. After rectification, times tacks were generated corresponding to the location of profile (figure 1(b)). A time stack represents the plotted evolution over time of a particular line of pixels. Morphological markers like the limit between sand and vegetation, or the limit formed by marine debris are easily identifiable on images and may be monitored overtime with time stacks. This latter has been identified and extracted on a daily basis. To obtain a runup value (Daily Highest Runup: DHR), the position of the swash limit on profile is correlated with the local Digital Elevation Model (DEM). The latter is derived from RTK-GPS monitoring. The position of the time stack extracted is presented on figure1.(b) present a mean pixel resolution on is 0.19 m.

Hydrodynamic data

Offshore wave conditions were extracted from the mesoscale MARC model outputs available online. MARC is a reanalysis of the WAVEWATCH III® model at a regional scale; simulation results are provided by the IFREMER and available in real time (http://umr-lops.org/marc). In order to compare the DHR obtained from the video system, daily maximum wave parameters were extracted from MARC model outputs. Actually, the daily H_s maximum value was extracted as well as Tp and Dp at the time of maximum wave height. A daily value of sea level from Pointe-à-Pitre tide gauge (figure 1(a)) was extracted following the same methodology. Data from the tide gauge are provided by the

French Hydrographic Service (SHOM) and available on the REFMAR database (www.http://data.shom.fr).

3. Results

Figure 2 presents observations over 1045 days. During this period, on MARC model dataset, offshore H_{rms} exceeded 3 m for 16 times, three of these events exceeded 4 m. The first was a winter storm with a peak on January 10th 2020 and the two others were cyclonic events peaking on July 20th 2020 and on September 20th 2020 related to Hurricane Teddy circulating at 800 km to the East of Guadeloupe Island. The latter was the most intense with maximum swash excursion of 12 m inland, and corresponding to runup exceeding 1.5 m. Figure 2 (c) presents the times tacks over the same period at cross-shore location represented by red line on figure 1 (b).

Seven major swash excursions events are easily identified on the time stack. The most extreme event was on September 17^{h} 2020, this event corresponds to the passage of Teddy Hurricane offshore Guadeloupe Island. All high runup events occurred during the cyclonic season and storms occurring during winter even the most extreme ones as the event number 4 in January 2020 seems to have not generated major swash excursion.

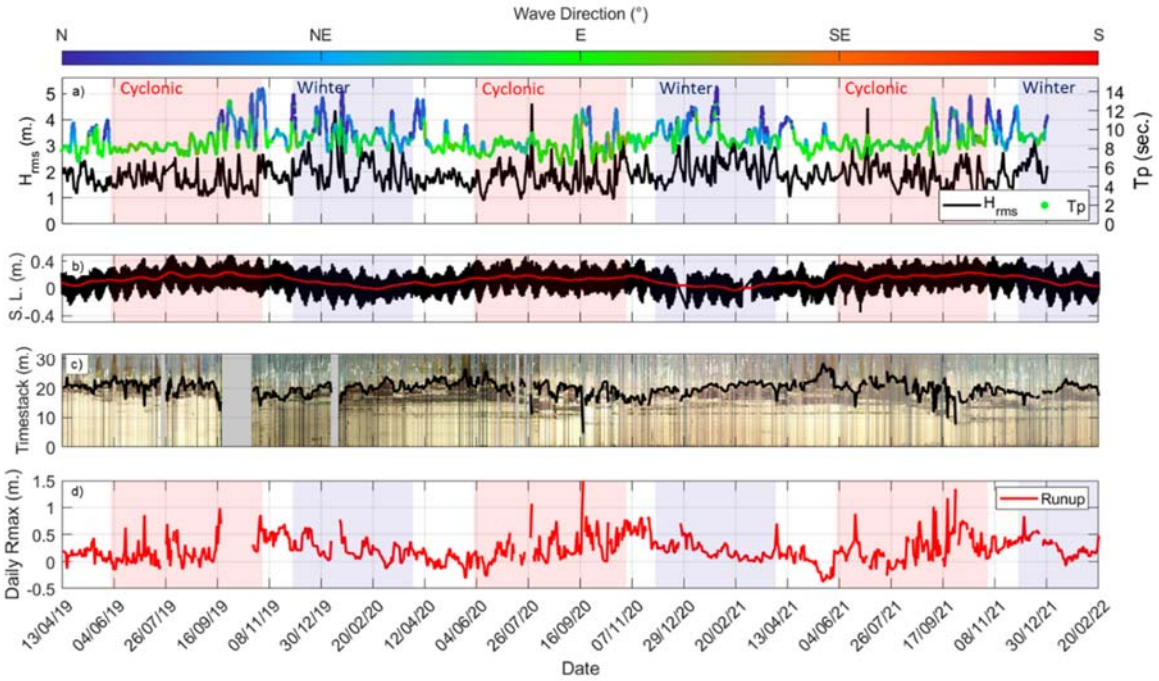

Figure 2. Incident wave and sea-level conditions and Camera derided observations from April 2019 to May 2021. (a) Offshore wave conditions on MARC model. (B) Sea-level variations on Pointe-à-Pitre tide gauge, 14 days moving mean is represented in red. (c) daily times tacks with detection of maximum swash limit (black line). (d) Evolution of the DHR on the profile.

As the DHR dataset showed great variations between seasons, it was decided to calculate annual cyclicity by applying a best fitting sinusoidal. The amplitude of the annual cycle (365.25 days/cycle) is estimated at 0.37 m, with a phase peak at day 309.5 (November 5th) with an R^2 of 0.48 with raw data, it represents 24% of the overall runup amplitude. In order to isolate the effect of sea level, storm periods were removed from the timeseries of DHR to remove the effect of storm surges and unusual waves. The method used by MASSELINK *et al.*, (2016) was applied to detect and isolate storms. On the H_s dataset, the percentile 95% $H_{s\,95\%}$ (here 2.3 m) was extracted and identified as storm peaks. The upcrossing and downcrossing on the 75% percentile defines the beginning and end of storms (here 1.84 m). Then, periods identified as storms were removed from runup dataset (see figure 3(b)). Some extreme runup events remain visible in particular around September 17th 2021. This may be due to an underestimation of waves by MARC Model, as the agitation is qualitatively validated by camera observation. The annual signal has now a phase peak at day 249.5, an amplitude of 0.18 m and a R^2 of 0.41 with the storm filtered runup signal, thus very close to sea level annual component (phase peak at day 247.6 and amplitude of 0.16 m (figure 3.d). Furthermore, when removing the annual cycle of sea level from the times series of the raw DHR, we obtained a runup signal that still shows an annual cyclicity with a phase of 335.5 days and 0.33 m amplitude. Figure 3(e) presents the evolution and annual cyclicity of wave power ($H_{rms}^2 * T_p$) in m²/s. The signal obtained fluctuates greatly and is very chaotic. The calculated annual periodicity shows bad skills with raw data (R^2 = 0.24) suggesting a better correlation with another periodicity. Nevertheless, the phase is 333.5 days, which is very close to the sea level filtered runup signal.

These results indicate that the DHR signal presents a strong annual seasonality. When main storms period is removed from the signal, the periodicity calculated on the residual is in phase with the effect of sea level annual variability, suggesting a strong modulation of runup by sea level annual seasonality. At the opposite, when this sea level variability is removed from raw runup, a good correlation between the residual annual periodicity and swell annual periodicity appears which may indicate a swell modulation as well on the runup. This double dependency of sea level and wave climate annual cyclicity on runup induces a periodicity to the runup with a specific phase

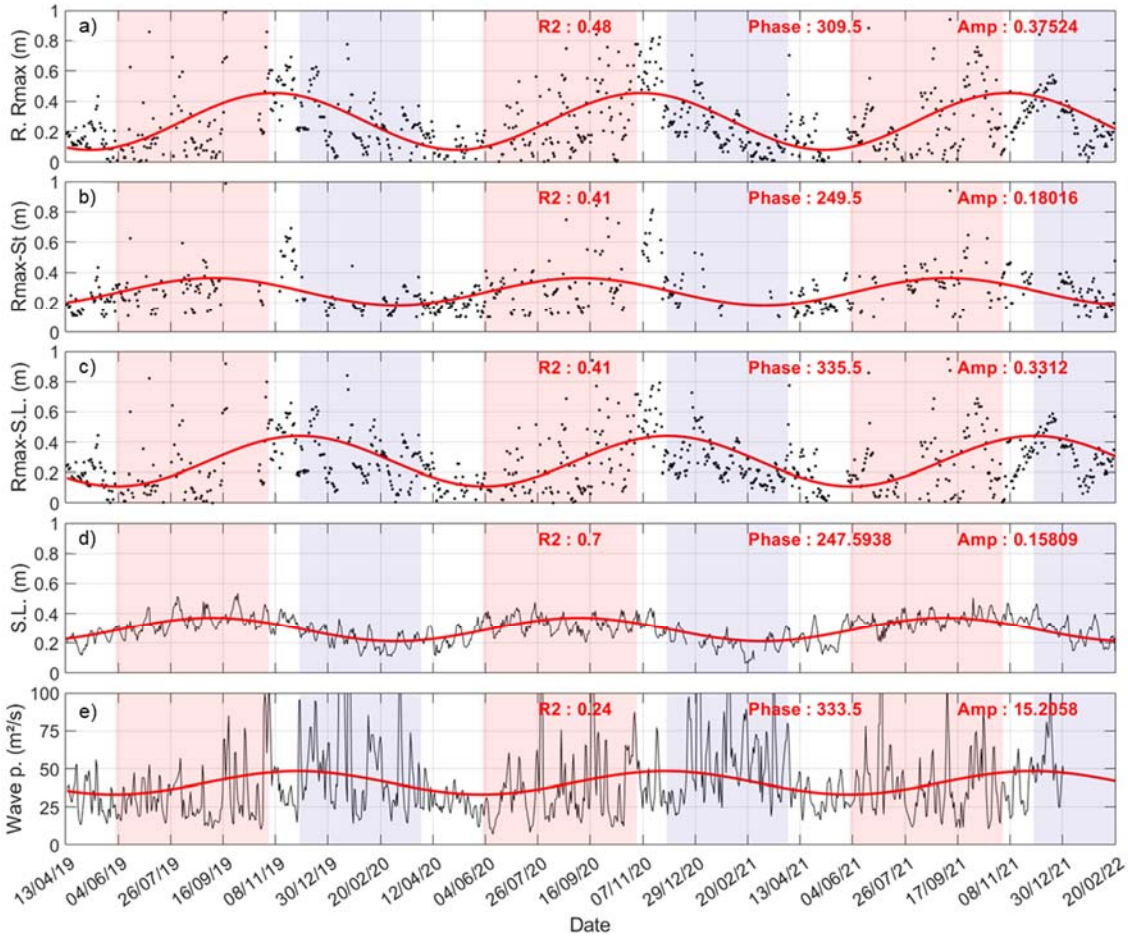

Figure 3. (a) Raw DHR observed on camera, (b) DHR with removal of storms periods, (c) DHR with removal of sea level annual periodicity, (d) Sea level with tide effect subtracted, (e) Wave power. Runup observation is plotted in black points, sea level and wave power in black line and annual periodicity in red line.

4. Discussion

4.1 Seasonal scale processes

Our results show a strong seasonal control on runup maximum elevation. However, this seasonality appears to be different from the seasonal oscillations of the water level, and from the seasonal variations of sea state in phase and amplitude. By retrieving sea-level seasonality from raw runup dataset, one finds the wave runup signal with a phase very close to sea state seasonality and vice versa. Wave climate periodicity is generated by both events mostly clustered on particular periods (winter and cyclonic seasons) and residual agitation (greater during winter) (REGUERO *et al.*, 2013). This cycle has an impact on runup periodicity as a similar pattern is found on runup signal with sea-level effect filtered. The effect of both cycles leads to an annual periodicity on runup with its own phase with minima in May and maxima in November.

In the context of Caribbean Islands and for the period of the study (e.g., 3 years), only the steric effect (TORRES & TSIMPLIS, 2012) seems to have a significant effect on sea level with an important spatial variability and approximately 15 cm amplitude at the study site location. Our results indicate that the effect of seasonal sea-level variation on runup and swash excursion is significant. This periodicity presents an amplitude of 0.37 m which represents 24% of the overall runup variability. During the low phase of the annual variability, which occurs in March, the effect of storms on runup is attenuated and during the high phase (peak) of the annual cycle occurring in October, storms of mild intensity may generate unexpected runup. Individual storms generate the highest runup values but are modulated by annual sea level periodicity.

4.2 Coral reef implication

The occurrence of a random wave event according to the annual periodicity will induce an overall mitigation or amplification of the induced runup (figure 3). The amplitude of the runup periodicity is greater than the amplitude of the water level periodicity. This may be explained by the presence of the coral reef. The steric expansion annual periodicity, acts on water depth and consequently on reef submergence. Coral reef wave filtering by wave breaking and bottom friction are dependent on water depth above the reef. Low water depth on the reef induces a high filtering of the swell while high water depth induces a lower filtering and a greater wave energy potentially reaching shoreline level. It also explains the lower runup variability observed during the low phases of sea level periodicity comparing to high phases. Such phenomenon is also observed on sandy beaches with sedimentary or rocky structures like bars (e.g. MELITO *et al*., 2022) but it is amplified in the presence of a coral reef in consequence of the steepness, high structural complexity and crest shallowness of such an environment. Moreover, even though it is not checkable with current dataset reef resonance could play a significant role in amplifying low frequency waves on the reef flat and thus on runup (PEQUIGNET et al., 2009; ROEBER and BRICKER, 2015; CHERITON et al., 2016). It could be trigger or not in function of incident wave group period and reef fundamental mode and generating seiche like undulations.

5. Conclusion

A camera-derived DHR timeseries over 1045 days from a reef-lined beach is presented. A strong annual periodicity was detected on the runup and appears to be linked to sea level annual variations generated by steric effect and to annual variations of wave climate. In the continuity of this study, several on site measurement campaigns were implemented to measure wave transformation through the reef and runup fluctuations on shorter timescales at a finer resolution and identify processes forcing the runup.

Acknowledgments

Thibault LAIGRE PhD thesis is undertaken within the EU Interreg Caribbean CARIB-COAST project.

6. References

AARNINKHOF S.G.J., RUESSINK B.G. (2004). *Video observations and model predictions of depth-induced wave dissipation*, in IEEE Transactions on Geoscience and Remote Sensing, vol. 42, no. 11, pp. 2612-2622, Nov. 2004, doi: 10.1109/TGRS.2004.835349.

CHERITON O.M., STORLAZZI C.D., ROSENBERGER K.J. (2016). *Observations of wave transformation over a fringing coral reef and the importance of low- frequency waves and offshore water levels to runup, overwash, and coastal flooding*. J. Geophys. Res. Oceans 121, 3121–3140. doi: 10.1002/2015JC011231

FERRARIO F., BECK M.W., STORLAZZI C.D., *et al*. (2014). *The effectiveness of coral reefs for coastal hazard risk reduction and adaptation*. Nat. Commun. 5, Article number: 3794. doi: 10.1038/ncomms4794

HARRIS, D. L., ROVERE, A., CASELLA, E., *et al.* (2018). *Coral reef structural complexity provides important coastal protection from waves under rising sea levels*. Sci. Adv. 4:eaao4350. doi: 10.1126/sciadv. aao4350

GUANNEL G., ARKEMA K., RUGGIERO P., *et al.* (2016). *The power of three: coral reefs, seagrasses and mangroves protect coastal regions and increase their resilience*. PLoS ONE 11(7): e0158094. doi:10.1371/journal.pone.0158094

KRIEN Y., DUDON B., ROGER J., *et al.* (2015). *Probabilistic hurricane-induced storm surge hazard assessment in Guadeloupe*, Lesser Antilles, Nat. Hazards

MASSELINK G., CASTELLE B., SCOTT T., *et al*. (2016). *Extreme wave activity during 2013/2014 winter and morphological impacts along the Atlantic coast of Europe*, Geophys. Res. Lett., 43, 2135–2143, doi:10.1002/2015GL067492.

MELITO L., PARLAGRECO L., DEVOTI S., *et al*. (2022). *Wave- and tide-induced infragravity dynamics at an intermediate-to-dissipative microtidal beach*. Journal of Geophysical Research: Oceans, 127, e2021JC017980. https://doi. org/10.1029/2021JC017980

MOISAN M., DELAHAYE T., LAIGRE T., *et al.* (2021). *Suivi des échouages de sargasse et de l'évolution du trait de côte par caméra autonome en Guadeloupe : analyse des résultats et bilan des observations*. Rapport final. BRGM/RP-712-FR, 67 p., 63 ill.

PEARSON S.G., STORLAZZI C.D., VAN DONGEREN A. *et al*. (2017). *A Bayesian-based system to assess wave-driven flooding hazards on coral reef- lined coasts*. J. Geophys. Res.: Oceans 122 (12), 10099–10117. doi: 10.1002/2017JC013204

PÉQUIGNET A.C.N., BECKER J.M., MERRIFIELD M.A., AUCAN J. (2009). *Forcing of resonant modes on a fringing reef during tropical storm Man-Yi.* Geophys. Res. Lett. 36:L03607. doi: 10.1029/2008GL036259

QUATAERT E., STORLAZZI C., VAN DONGEREN, A., *et al.* (2020). *The importance of explicitly modelling sea-swell waves for runup on reef-lined coasts*. Coastal Eng. 160:103704. doi: 10.1016/j.coastaleng.2020. 103704

REGUERO B.G., MÉNDEZ F.J., LOSADA I.J. (2013). *Variability of multivariate wave climate in Latin America and the Caribbean Global Planet Change*, 100, pp. 70-84

ROEBER, V., BRICKER, J.D. (2015). *Destructive tsunami-like wave generated by surf beat over a coral reef during Typhoon Haiyan.* Nat. Comm. 6:7854. doi: 10.1038/ncomms8854

RUEDA A., VITOUSEK S., CAMUS P., *et al.* (2017). *A global classification of coastal flood hazard climates associated with large-scale oceanographic forcing*. Sci Rep 7, 5038 https://doi.org/10.1038/s41598-017-05090-w

SHOM - Service Hydrographique et Océanographique de la Marine. (2020). *Références Altimétriques Maritimes*, édition 2020. 126p.

TORRES R.R., TSIMPLIS M.N. (2012). *Seasonal sea level cycle in the Caribbean Sea,* J. Geophys. Res., 117, C07011, doi:10.1029/2012JC008159.